REFERENCES

1. Brinker, C. J.; Scherer, G.W., *Sol-Gel Science*. Academic Press, San Diego, 1990.
2. Livage, J.; Beteille, F.; Roux, C.; Chatry, M.; Davidson, P., *Acta Mater.*, **1998,** *46(3)*, 743.
3. Caroline, M. P.; James, A. R.; Michael, D. A., *J. Non-Cryst. Solids*, **2001,** *279*, 119.
4. Perry, C.C.; Li, X.; Waters, D.N., *Spectrochim. Acta,* **1991,** *47A*,1487.
5. Lopez, T.; Asomaza, M.;Gomez, R., *J. Non-Cryst. Solids,* **1992**, *147&148*, 769.
6. Lopez, T; Asomaza, .M.; Bosch, P; Garcia-Figueroa, E.; Gomez, R. *J. Catal.*, **1992,** *138*, 463.
7. Livage, J.; Henry, M.; Sanchez, C., *Progr. Solid State Chem.*, **1988,** *18*, 259.
8. Livage, J.; Sanchez, C.;. Henry, M; Doeuff, S. *Solid State Ionics*,**1989**, *32/33*, 633.
9. Sanchez, C.; Livage, J., *New J. Chem.*, **1990,** *14*, 513.
10. Fitremann, J.; Doeuff, S.; Sanchez, C., *Ann.Chim. Fr.*, **1990,** *15*, 421.
11. Hence L.L.;. West, J. K., *Chem. Rev.*, **1999,** *90*, 33.
12. Hu, M.Z.C.; Zielke, J.T.; Byers, C.H.; Lin, J.S.; Harris, M.T., *J. Mater. Sci.,* **2000**, 1957.
13. Huling, J.C.; Messing, G.L., *J. Non-Cryst. Solids,* **1992**, *147&148*, 213.
14. Schneider, H.; Saruhan, B.; Voll, D.; Merwin, L.; Sevald, A., *J. Eur. Ceram. Soc.*, **1993**, *11*, 87.
15. Guizard, C.; Cygankiewcz. N.; Larbot, A.; Cot. L., *J. Non-Cryst. Solids,* **1986,** *82*, 86.
16. Debsikdar, J.C., *J. Non-Cryst. Solids,* **1986**, *86*, 231.
17. Mehrotra, R.C.; Anirudh Singh., *Prog. Inorg. Chem.*, **1997**, *46*, 239.
18. Turevskaya, E.P.; Kozlova, N.; Shreider, V.; Ya Turova, N., *Inorg. Chim. Acta.,* **1981**, *53*, 573.
19. Suzuki, E.; Kusano, S.; Hatayama, H.; Okamoto, M.; Ono, Y., *Chem. Mater.*, **1997**, *7*, 2049.

20. Kemmitt, T.; Al-Salim, N.I.; Gainsford, G.J.; Henderson, W., *Aust. J. Chem.*, **1999**, 52, 10915; T.

21. Laine, R.M.; Blohowiak, K.Y.; Robinson, T.R.; Hoppe, M.L.; Nardi, P.; Kampf, J.: Uhm, J., *Nature,* **1991**, *353*, 642.

22. Blohowiak, K.Y.; Laine, R.M.; Robinson, T.R.; Hope, M,L.; Kampf, J.I., *Inorganic and Organometallic Polymers with Special Properites*; ACS: Netherland, 1992.

23. Bickmore, C.;Hoppe, M.L.; Laine, R.M., *Mat .Res. Soc. Symp. Proc.*, **1992**, *249*, 81.

24. Jitchum, V.; Chivin, S.; Wongkasemjit S.; Ishida, H., *Tetrahedron,* **2001**, *57*, 3997.

25. Laine, R.M.; Youngdahl, K.A.; Nardi, P. Washington Research Foundation, U.S. Pat. No.5,099,052, 1992.

26. Laine, R.M.; Youngdahl, K.A. Washington Research Foundation, U.S. Pat. No. 5,216,155, 1993.

27. Gainsford, G.J.; Kemmitt, T.; Milestone, N.B., *Inorg. Chem.,* **1995**, *34*, 5244.

28. Gainsford, G.J.; Kemmitt, T.; Lensink, C.; Milestone, N.B., *Inorg. Chem.,* **1995**, *34*, 746.

29. Wang, D.; Yu, R.; Kumada, N.; Kinomura, N., *Chem. Mater.,* **1999**, *11*, 2008.

30. Wongkasemjit, S.; Laine R.M.; Piboonchaisit, P., *J.Sci.Res.Chula.Univ.*, **2001,** *26(2),* 95.

31. Opornsawad, Y.; Ksapabutr, B.; Wongkasemjit, S.; Laine, R.M., *Eur. Polym. J.*, **2001,** *37/9*, 1877.

32. Charoenpinikarn, W.; Suwankuruhasn, M; Kesapabutr, B.; Wongkasemjit, S. ; Jamieson, A.M., *Eur. Polym. J.*, **2001**, *37/7*, 1441.

33. Piboonchaisit, P.; Wongkasemjit, S.; Laine, R., *Science-Asia, J. Sci. Soc. Thailand*,**1999,** *25*, 113.

34. Guizard, C.G.; Julbe, A.C.; Ayral, A., *J. Mat. Chem.*, **1999,** *9*, 55.

35. Spilliman, R., *Membrane Separations Technology. Principles and Applications* Noble, R. D.; Stern de, S.A., Elsevier, **1995**, 589

36. Klein, L.C., *Sol-Gel Technology for Thin films, Fibers, Preforms, Electronics, and Specialty Shapes*, Noyes, Park Ridge, New Jersey, 1988.

37. *Encyclopedia of Chemical Technology*, Volume 22 (4th ed.), Wiley-Interscience.
38. Hench, L.L., West, J.K., Chem. Rev., **1990**, *90*, 33
39. Yi, G., Sayer, M., Ceram. Bulletin., **1991**, *70*, 1173
40. Pouskouleli, G. *Ceram, Int.*, **1989**,*15*, 255.
41. Sakka, S.; Kamiya, K., *J. Non-Cryst. Solids,* **1980**, *42*, 403.
42. Ding, X.; Qi, Z.; He, Y., *J. Mater. Sci. Lett.*, **1995,** *14* , 21.
43. Duran, A.; Serna, C.; Fornes, V.; Fernanedez Navarro, J., *J. Non-Cryst. Solids* **1986**, *82*, 69.
44. Bradley, D.C., Mehrotra, R.C., Gaur, D.P., Metal Alkoxides, Academic Press, London, 1978.
45. Bradley, D.C., Chem. Rev., **1989**, *89*, 1317.
46. Doeuff, S.;. Dronzee, Y; Tautelle, F.; Sanchez, C., *Inorg. Chem.*, **1989**, 28, 4439.
47. Chandler, C.; Roger, C.; Hampden-Smith, M., *Chem. Rev.*, **1993,** *93*, 1205.
48. Bickmore, C.; Laine, R., *J. Am. Ceram.Soc.*, **1996,** *79*, 2865.
49. Voronkov, M.G.; Zeltschan, G.I., *Chem.Abstr.*, **1956**, *63*, 328.
50. Mehrotra, R.C.; Mehrotra, R.K. *J,. Indian Chem.Soc.*, **1962**, *39*, 677.
51. Thomas, W.M.; Groszos, S.J.; Day, N.E. *U.S.Patent* 2,985,685, **1961**; *Chem.Abstr.*, **1961**,*55*, 20966.
52. Hein, Fr.; Albert, P.W. Z., *Anorg.Chem.*, **1952**, *269*, 67.
53. Icken; J.M.; Jahren, E.J.*Chem. Abstr.*, **1968**, 60, 2768.
54. Stanley, R.H. *British Patent* 1,123,559, **1968** ; *Chem.Abstr.*, **1968,** *69*, 78532.
55. Elbing, I.N.; Finestone, A.B., *Chem. Abstr.*, **1964**, *60*, 14705.
56. Higashi, H.; Namikawa, S., *Chem. Abstr.*, **1968**, *68*, 13474.
57. Frye, C.L., *J. Org.Chem.*, **1969**,*34*, 2496.
58. Frye, C.L.; Vincent, G.A.; Finzel, W.A., *J.Am. Chem.Soc.*, **1971**, *93*, 6805.
59. Frye, C.L., *J. Am.Chem.Soc.*, **1970**, *92*, 1205.
60. Laine, R.M.; Mueller, B.L.; Hinklin, T., *U.S.Patent No.* 5,418,298, May 23, **1995**.

APPENDICES

Appendix A

FORMATION AND STRUCTURE OF TRIS(ALUMATRANYLOXY-I-PROPYL)AMINE DIRECTLY FROM $Al(OH)_3$ AND TRIISOPROPANOLAMINE

Abstract

Recently, a new one step method was developed for synthesizing a methyl substituted alumatrane directly from aluminum hydroxide [$Al(OH)_3$] and triisopropanolamine (TIS). The structure of TIS-Al was characterized using DSC, TGA, FAB^+-MS, NMR (^1H-, ^{13}C-, ^{27}Al-) and FTIR. Triethylenetetramine (TETA), a stronger base than TIS, was found to act as a catalyst to accelerate the $Al(OH)_3$ dissolution rate. The kinetics of TIS-Al formation were studied as a function of different condition. The activation energy of reaction was 24 ± 2 kJ mol^{-1}.

Introduction

Atranes, I, with M=B, Al, Si, Ge, Sn, Pb, P, Ti, V, Mo, etc. have been synthesized and studied extensively over the last three decades [1-5]. These compounds are of interest owing to their cage structure and physical/chemical properties. The behavior of alumatrane, where M=Al, 2,8,9-trioxa-5-aza-1-alumatricyclo [$3.3.3.0^{1,5}$] undecane, and oligomeric alumatrane has been described previously [6-7]. In benzene, cryoscopy, and ebullioscopy indicate tetrahedral and octahedral behavior. A mass spectroscopic (EI 70 eV) study showed the stability of the dimer I′ in the gas phase.

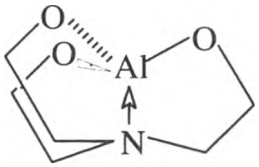

I

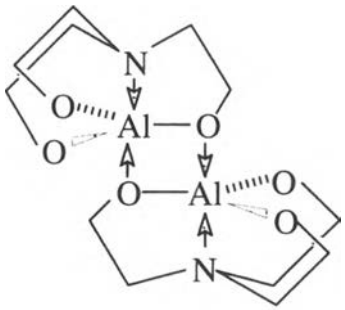

I′

There are several methods of preparing alumatranes. Alumatrane is prepared readily in high yield by reaction of aluminum alkoxides with triethanolamine in an aromatic solvent [10,11] or with no solvent [12-14]. Triethylaluminum also reacts with triethanolamine in toluene or hexane at -78 °C to form alumatrane [15]. Verkade [16] prepared alumatrane by the alcoholysis of tris-(dimethylamido) aluminum with triethanolamine and also by transligation of monomeric and dimeric alumazatranes with triethanolamine.

According to ^{27}Al-, ^{1}H-, and ^{13}C-NMR data, they found tetramers, II, in solution and dimeric I′ by mass spectra in the gas phase. Alumatrane precursors, aluminum alkoxide [$Al(OR)_3$] or aluminum alkyl [$Al(R)_3$] are expensive and the syntheses are multistep. Laine et al. have developed an inexpensive way to convert metal oxide or hydroxides, namely, $Al(OH_3)$ and silica, into novel materials ranging from ion conducting [17], liquid crystalline polymers [18], to oligomeric and polymeric precursors [19].

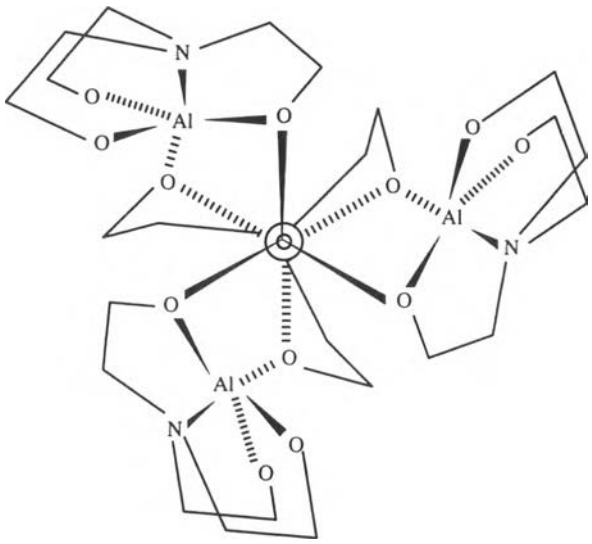

II

Laine also found that higher boiling point amine bases (b.p. >200 °C), such as triethanolamine and triethylenetetramine (TETA) can be used either in catalytic or stoichiometric quantities to dissolve SiO_2. Moreover, they also found that approximately stochiometric quantities of triethanolamine will effectively dissolve $Al(OH_3)$. The "oxide one pot synthesis process (OOPS)" for alkoxyalanes was developed after it was discovered that stochiometric amounts of triethanolamine would dissolve $Al(OH_3)$, the source matrial for most pure alumina.

The purpose of this work is to extend previous efforts to reactions of $Al(OH_3)$ and triisopropanolamine (TIS), and study the kinetic of the product formation, which includes the reaction order, rate constant, and activation energy. Along with this, the effect of TETA on the reaction was also studied to improve the solubility of this novel aluminum alkoxide in non-polar solvents for use as a catalytic intermediate in sol-gel processing

Experimental section

Materials. The starting materials and products are slightly moisture and air sensitive. Therefore, all operations were carried out with careful exclusion of air by purging with nitrogen gas.

UHP grade nitrogen; 99.99% purity was obtained from Thai Industrial Gases Public Company Limited (TIG). Aluminum hydroxide hydrate [$Al(OH)3{\cdot}xH_2O$] containing 57.5 % Al_2O_3 as determined by TGA was purchased from Aldrich Chemical Co. Inc. (USA) and used as received. Ethylene glycol (EG), used as solvent in the reaction, was purchased from Farmitalia Carlo Erba (Barcelona) and purified by fractional distillation at 200 °C, under N_2 before use. TIS was obtained from Fluka Chemika-BioChemika (Switzerland) and used as received. TETA was obtained from Union Carbide Thailand Limited (Bangkok, Thailand) and distilled under vacuum (10^{-2} Torr) at 120 °C. Acetonitrile and methanol were purchased from J.T. Baker Inc. (Philipburg, USA) and purified by standard techniques.

Instrumentation. Mass spectra were obtained on a 707E-Fison Instrument (VG-Autospec, Manchester, England) with a VG data system, used in the positive fast atomic bombardment (FAB^+) mode. Thermal analysis was carried out on a Netzsch DSC 200 (Germany) and a Netzsch Gerätebue BmbH Thermal analysis TG 209 (Germany). ^1H- and ^{13}C-NMR spectra were obtained using a 500 MHz JEOL (JNM-A500) spectrometer at the Scientific and Instrumental Research Equipment Center, Chulalongkorn University, using deuterated methanol (CD_3OD) and tetramethysilane (TMS) as the solvent and internal reference, respectively. ^{27}Al-NMR spectra were recorded on Bruker 360 MHz at the University of Michigan. Fourier transform infrared (FTIR) spectra were recorded on a Bio-Rad FT-45A FTIR spectrometer with a resolution of ±4 cm^{-1}.

Procedure. General procedures to obtain tris(alumatranyloxy-*i*-propyl)amine are as follows; aluminum hydroxide, 50 mL of EG, and TIS were added to a 250 mL two-necked round bottomed flask. The reaction mixture was stirred and heated under N_2 in a thermostatted oil bath. When the oil bath temperature reached 200°C, the reaction was considered to have commenced. Fresh EG in the same amount as the distillate was added to maintain the total reaction volume until the reaction mixture turned clear (about 3 hour), indicating reaction completion. After letting the reaction mixture stand without stirring overnight,white product precipitated out.

After filtering, the product was stirred with dried acetonitrile overnight to remove excess TIS. The solid product was then filtered off and dried under high vacuum (10^{-2} torr) at 120°C for 5 h. Dried products were then characterized using DSC, TGA, FTIR, FAB^+-MS and NMR.

Unreacted alumina recovered from a reaction was purified as follows: after the reaction mixture was cooled, unreacted $Al(OH)_3$ was filtered off, and stirred with dried methanol overnight to extract remaining product from unreacted $Al(OH)_3$. The unreacted $Al(OH)_3$ was filtered off, washed with 2 x 20 ml of dried methanol, and then oven dried at 120 °C for 10 h. Finally, the dried $Al(OH)_3$ was calcined in the TGA to obtain the alumina content. The total unreacted $Al(OH)_3$ was recalculated to obtain reacted alumina.

Kinetic studies. The kinetic studies were primarily conducted on the dissolution of $Al(OH)_3$ as a function of changes in the reaction conditions, namely, the amount of TIS, the amount of aluminum hydroxide, reaction temperature, and time. Each reaction was repeated three times.

The optimum ratio of TIS was studied by fixing the amount of $Al(OH)_3$ (57.5% Al_2O_3 content by TGA) at 22.7 mmol or 10 mmol equivalent of Al_2O_3. The amount of TIS was varied from 0-50 mmol. The reaction time and temperature were fixed at 3 h and 200°C, respectively.

Dissolution Rate as a Function of $Al(OH)_3$ Concentration. The amount of TIS was fixed at 3.83 g (20 mmol) and the amount of $Al(OH)_3$ was varied from 0.89-8.87 g (5-40 mmol). EG was added to make the total volume of reaction mixture 50 mL. The reaction time and temperature were set at 1 h and 200°C, respectively. Each run was repeated three times. The relationship between mmol of unreacted alumina and mmol of alumina added was plotted.

Dissoluion Rate as a Function of TETA Concentration. To study the effect of [TETA] on the rate of reaction, $Al(OH)_3$ and TIS quantities were fixed at 1.77 g (22.7 mmol) and 0.96 g (5 mmol), respectively. The concentration of TETA

was varied from 0-4.3875 g (0-30 mmol). The reaction time and temperature were fixed at 3 h and 200°C. The relationship between mmol dissolved alumina and mmol TETA added was then plotted.

Determination of the Reaction Rate Constant and Activation Energy. Amounts of $Al(OH)_3$ and TIS were fixed at 1.77 g (22.7 mmol) and 0.96 g (5 mmol), respectively. The reaction time was varied from 15-120 min with increments of 15 min at 150°, 170°, 190°, and 200°C. The relationship between mmol of unreacted alumina versus reaction time at each reaction temperature was then plotted to obtain the reaction rate constant (k). The activation energy was then calculated by plotting ln (k) versus 1/T (1 K^{-1}).

Dissolution Rate as a Function of Time in the Presence of TETA as a Catalyst. The effect of time on the reaction of $Al(OH)_3$ and TIS with TETA as a catalyst was studied by fixing the amounts of $Al(OH)_3$, TIS, and TETA at 1.77g (22.7 mmol), 0.96 g (5 mmol), and 0.18 g (1.25 mmol), respectively. The reaction temperature was fixed at 200°C and the reaction time was varied from 15-120 min. The mmoles of unreacted alumina for each run were then plotted versus time.

Results and discussion

In this study, recovered $Al(OH)_3$ was thermally converted to α-alumina to determine the actual amount dissolved. $Al(OH)_3$ used at the beginning and left after the reaction was measured as Al_2O_3 using TGA ceramic yield.

As seen in Fig. 1., with a fixed amount of aluminum hydroxide hydrate [1.77 g (22.7 mmol)] at a reaction time and temperature of 3 h. and 200 °C, respectively, the reaction went very slowly for TIS quantities less than 20 mmol. However, it went to completion when 35 mmol of TIS was used. It was found also that when 10 mmol of TETA was used with the 22.7 mmol of $Al(OH)_3$ and 35 mmol of TIS, the reaction was complete within 2 h. (see Fig. 6).

Dissolution rate as a function of $Al(OH)_3$. In this case, determination of a reaction rate, the so-called "method of initial rates", was based upon an accurate analysis of one product at a very early stage of reaction. Therefore, all reactions studied did not proceed to completion. The reaction time and temperature were thus set at 1 h and 200°C. The amount of alumina was varied from 7.5 to 12.5, 15, and 40 mmol while the concentration of TIS was fixed at 20 mmol. The relationship between the dissolved and added alumina is nearly linear, (Fig. 2). Clearly, the reaction of $Al(OH)_3$ and TIS also depended on the concentration of $Al(OH)_3$. The curve was nearly linear, suggesting that the reaction was first order with respect to $Al(OH)_3$ and first order with respect to TIS. It is worth noticing that the intercept of both curves are not equal to zero. This is because some unreacted $Al(OH)_3$ is lost during recovery step.

Determination of the reaction rate constant and the activation energy.

We used the integral method to determine the reaction order. The reaction order was assumed to be second order overall. Plots of ln[(1-rX)/(1-X)] versus reaction time at each temperature are presented in Fig. 3, (note: the linearity of the data suggesting that the reaction is most likely to be second order as assumed). The reaction rate constants were obtained from the slope of the plotted data, straight line with different gradients. As expected, the higher temperature showed the higher gradient, meaning that the higher reaction temperature, the higher dissolution rate.

To determine the activation energy, the Arrhenius equation was employed. From section 3.2.3, after obtaining the reaction rate constants (k), ln k was plotted versus 1/T(1/Kelvin) as Fig. 4, which gives a straight line with the slope proportional to the activation energy. The slope obtained is equal to the activation energy devided by the gas constant (8.314 J mol^{-1} K^{-1}). As a result, the activation energy was 24±2 KJ mol^{-1}.

Dissolution Rate as a Function of TETA Concentration. The plot of the amount of dissoved $Al(OH)_3$ and amount of TETA is presented in Fig. 5. The higher the TETA concentration, the greater the amount of dissolved $Al(OH)_3$. At low TETA concentration (1.25-2.5 mmol), the amount of $Al(OH)_3$ dissolved increased

significantly, as compared to the higher TETA concentrations. This is due to the role of TETA acting as solubilization catalyst to increase the surface area of $Al(OH)_3$.

Dissolution rate as a function of time in the presence of TETA as a catalyst. Fig. 6 shows a plot of mmol of unreacted $Al(OH)_3$ versus reaction time comparing reactions with and without TETA. The dissolution reaction rate with TETA was faster than that without TETA because TETA increased solubility of $Al(OH)_3$, resulting in increasing its surface area which caused the reaction to go faster, as discussed previously.

Characterization

Thermogravimetric Analysis. The TGA data for the product from the reaction without TETA shows two major regions of mass loss (Fig.7 (a)). The first region was between 180°-260°C that indicated the decomposition of TIS which is a component of the product while the second region occurred at about 260°-550°C which corresponded to the oxidative decomposition of the organic ligands and carbon residues. The % ceramic yield of the product was 27.6 %, which was higher than the theoretical ceramic yield (23.7 %) owing to the incomplete combustion of the sample since the final ash was still gray in color.

Similarly, the TGA of the product synthesized in the presence of TETA (Fig .7(b)) also showed two major mass losses at 180°-250°C and 250°-500°C corresponding to the decomposition of TIS ligand and the oxidative decomposition of the organic ligands, and carbon residues, respectively. The % ceramic yield of product was 31.9 %, which was much higher than the theoretical yield. This can be explained along with the mass spectrum which indicated that the product synthesized from the batch with TETA gave more dimer (m/e 431) than the one without TETA because mass spectral data showed that the product consists of monomer, trimer, pentamer, and hexamer. The more smalller unit, the higher ceramic yield. Moreover, the final ash was darker in color.

Differential Scanning Calorimetry. The DSC of the product from the reaction without TETA, see Fig. 8(a), showed an exotherm at 250°-280°C corresponding to the boiling point of TIS, since when the product was run the second time, there was no exothermic peak in DSC thermogram. An endotherm at 380°-400°C, as compared to its TGA, correlated to the decomposition temperature of products. The T_g was observed at about 167°C.

Similarly, the DSC data of the product from the reaction with TETA, as shown in Fig. 8(b), indicated the exotherm at about 220°-260°C corresponding to the meltingpoint followed by the decomposition of the product, the endotherm at about 350°-380°C. It is worth noticing that the both temperatures are lower than those in Fig. 8(a). This is due to the more smaller units containing in the products obtained from the reaction with catalyst TETA. The T_g of this product occured at about 166°C.

Positive fast atomic bombardment mass spectroscopy. Mass spectral analysis suggests that there are four different alumatrane complexes; hexamer (m/e 1292), the highest intensity pentamer plus one morpholine (m/e 1250), resulted from losing a molecule of water in TIS, trimer plus one ethylene glycol (m/e 707), and monomer plus one TIS (m/e 409) and the intensities of all proposed structures was shown in table 1.

The fragmentation pattern of the product from the reaction with TETA gave higher intensities of the lower unit peaks at m/e 216 and 409, and lower intensity of the peak at m/e 1250. This result can obviously confirm that the reaction carried out without TETA gives the product containing higher molecular weight unit than the one run with TETA owing to the acceleration of TETA resulting in faster completion of the reaction.

Nuclear magnetic resonance spectroscopy

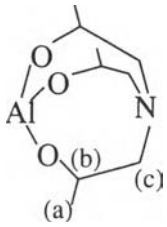

The NMR results showed that the products certainly contained several kinds of oligomers, such as monomer, dimer, etc., which are coincided with the mass spectroscopy results. The ^{1}H-NMR spectrum of the product from the reaction without TETA showed three multiple characteristics of quadrapolar coupling peaks indicating the presence of a few species in the product. The peaks at 1.1-1.4 ppm correspond to the -CH_3 group of TIS, position (a). The peaks at 2.4-3.1 ppm are assigned to the methylene group adjacent to the N-atom of TIS (-N-CH_2) at position (c). The peaks at 3.6-4.2 ppm are assigned to the tertiary carbon adjacent to the O-atom of TIS, position (b). The ^{1}H-NMR spectrum of the product from the reaction with TETA gave a similar one.

Similarly, the ^{13}C-NMR spectrum of the product from the reaction without TETA showed a multiple peak at 22.0 ppm corresponding to -CH_3 groups at position (a) coupled to itself and proton of the tertiary carbon. The sharp peak at 64.3 ppm belongs to the carbon adjacent to N-atom of TIS (-N-CH_2) at position (c). The multiple peak at 79.0 ppm is associated with the carbon adjacent to O-atom of TIS (position (b)) due to the coupling with -N-CH_2 and -CH_3. The spectrum of both reactions showed the similar positions.

The ^{27}Al-NMR spectra of the products from the reaction with and without TETA coincidentally showed 3 multiple peaks, as shown in Table 3.2, at around 65, 49 and 7 ppm at the ratio of 1:1:1. Again, these three peaks indicated the presence of both hexa- (at 7 ppm) and tetracoordinated (at 65 and 49 ppm) aluminum compounds.

Fourier Transform Infrared Spectroscopy. The FTIR spectra of the products from the reactions with and without TETA show similar functional groups (Table 3). Due to the moisture sensitivity of the products, the ν O-H appears at 3300-3700 cm^{-1}, and the wave number at 2750-3000 cm^{-1} corresponds to ν C-H. The single peak at about 1650 cm^{-1} is O-H overtone and C-H bending. The strong peak at 1000-1250 cm^{-1} results from the ν C-N and/or O-H bending. The broad peak at 500-800 cm^{-1} represents the ν Al-O of the product.

Conclusions

In this work, alumatrane complexes were synthesized directly from inexpensive starting material, aluminum hydroxide, and TIS, via the one step process, called "OOPS" process. Mass spectra revealed that products were oligomers. The main product was pentamer bonded with TIS that lost one H_2O molecule. From TGA data, the % ceramic yields of the product from the reactions without and with TETA were 27.6 and 31.9 %, respectively, which are higher value than the theoretical yield (23.7%). The higher percent ceramic yields were due to the small unit of oligomers in the product and the small amount of unreacted $Al(OH)_3$ remaining in the product.

The reaction order was second order overall, first order with respect to aluminum hydroxide and first order with respect to TIS. The dissolution rate increased when the reaction temperature increased. The activation energy of this reaction was about 24±2 KJ mol^{-1}.

Acknowledgements

This study was funded by the National Research Council of Thailand and Thailand Research Fund.

References

1. Voronkov, M. G., Seltschan, G. I., Lapsina, A. and Pestunovitsch, V. A., ***Z. Chem.,* 1968,** 8.
2. Voronkov, M. G., *Vestnik Akad. Nauk SSSR*, 1968, 38, 48
3. Voronkov, M. G. and Zelchan, G. I., *Khim. geterotsikl. soed.*, 1965, 51.
4. Bradley, D. C., Mehrotra, R. C., Gaur, D. P., *Metal Alkoxides;* Academic Press: N. Y., **1978,** 266.
5. Pinkas J., Verkade G., *Inorg. Chem.*, 1993:32:2711.
6. Hein, F. and Albert, P. W. Z., *Anorg. Allg. Chem.,* **1952,** 269, 67.
7. Mehrontra, R. C. and Mehrotra, R. K., *J. Indian Chem. Soc.,* **1962,** 39, 677.
8. Mehrotra and Rai, A. K., *Polyhedron,* **1991,** 10, 1967.
9. Shklover, V. E., Struchkov, Yu. T., Voronkov, M. G., Ovchinnikova, Z. A. and Baryshok, V. P., *Dokl. Akas. Nauk (Engl. Transl),* **1984,** 227, 723.
10. Voronkov, M.G., Baryshok, V.P., *Organomet. Chem.*, **1982**:239:199.
11. Thomas, W. M., Groszos, S. J and Day, N. E., U.S. Patent 2, **1961,** 985, 685; *Chem. Abstr.,* **1961,** 55, 20966.
12. Icken, J. M. and Jahren, E. J., *Belg. Patent 619,* 1963, 940; *Chem. Abstr.,* **1963,** 60, 2768.
13. Stanley, R. H., *British Patent 1,* **1968,** 123,559; *Chem. Abstr.,* **1968,** 69, 78532.
14. Elbing, I. N. and Finestone, A. B., *German offen 1.,* **1964,** 1,162,439; *Chem. Abstr.,* **1964,** 60, 17/4705.
15. Higashi, H. and Namikawa, S., *Kogyo Kagaku Zasshi,* **1967,** 70,97.
16. Verkade, J. K., *Acc. Chem. Res.,* **1993,** 26, 483.
17. Blohowiak, K., Tradewell, D., Mueller, R., Hoppe, M., Jouppi, S., Kansal, P., Chew, K.W., Scotto, C., Babonneau, F., Kampf, J. and Laine, R.M., *Chem. Mater.*, **1994**:6:2177-92
18. Ray, D. G., Laine, R. M., Robinson, T. R., Viney, C., *Mol. Crys. Liq. Crystal,* **1992**, 225,153.
19. Laobuthee, A., Wongkasemjit, S., Traversa, E. and Laine, R., *J. Eur. Cer. Soc.*,**2000**, 20,185-191.

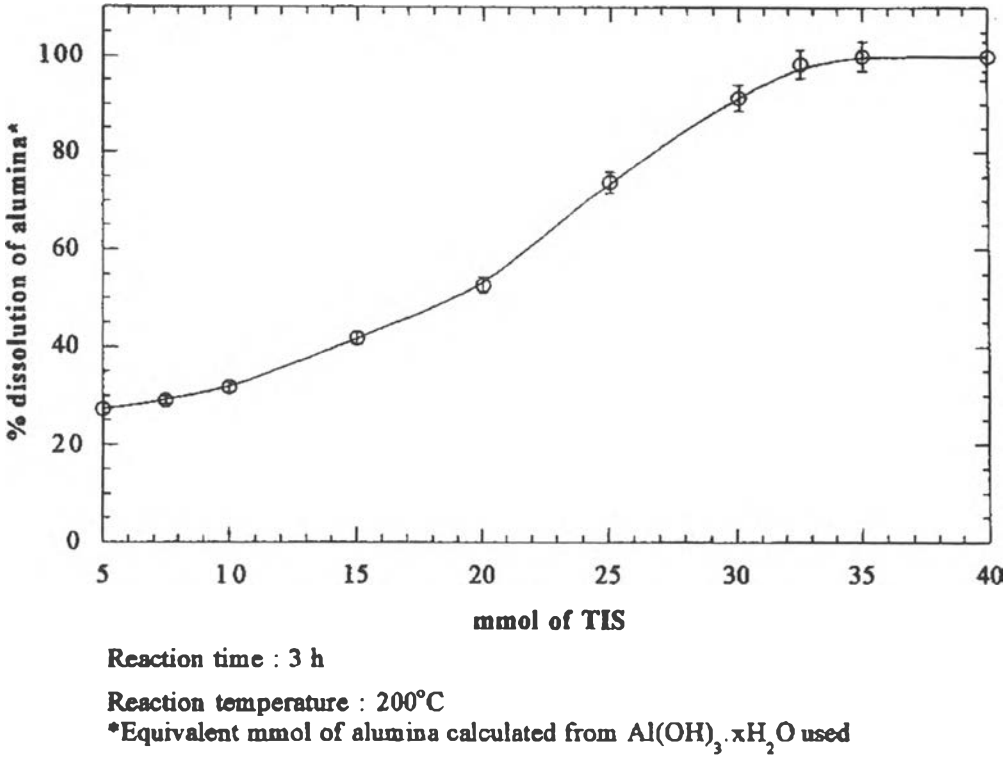

Figure 1 Optimization of $Al(OH)_3$:TIS ratio for complete $Al(OH)_3$ dissolution.

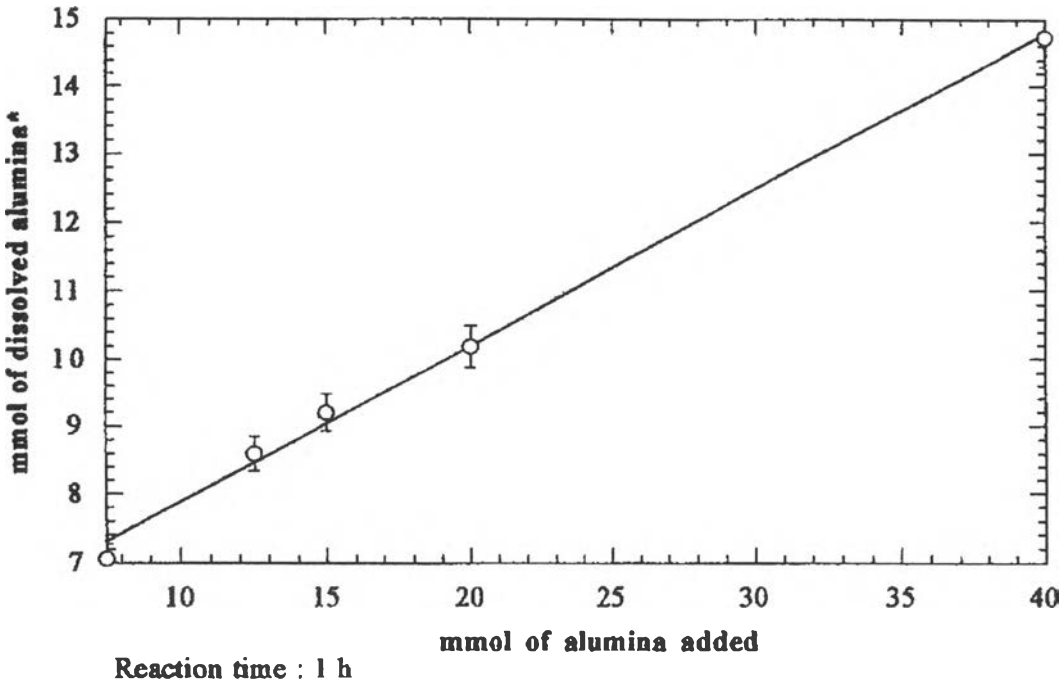

Figure 2. Dissolution rate as a function of $Al(OH)_3$ concentration.

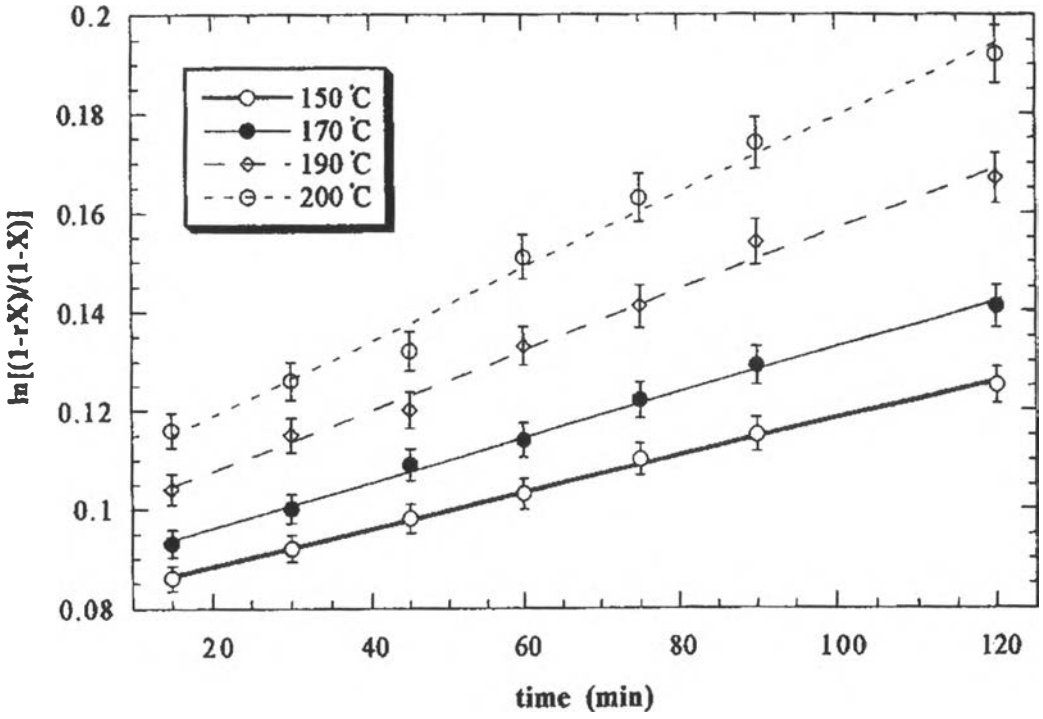

Figure 3. The relationship of logarithm of conversion factor versus reaction time for each variation of reaction temperature.

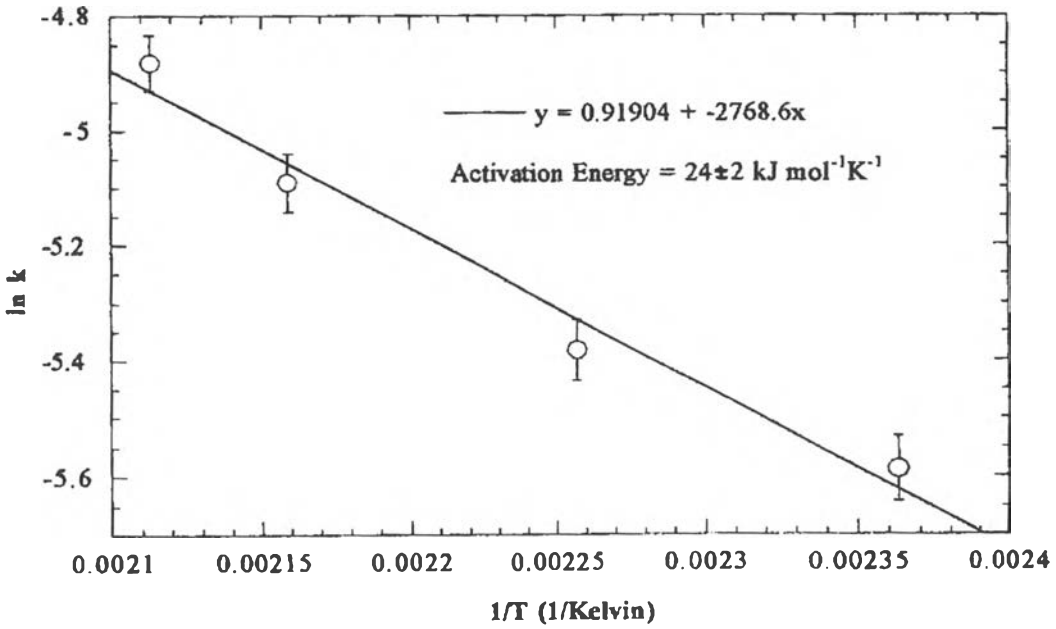

Figure 4. The relationship of logarithm of rate constant and reaction temperature.

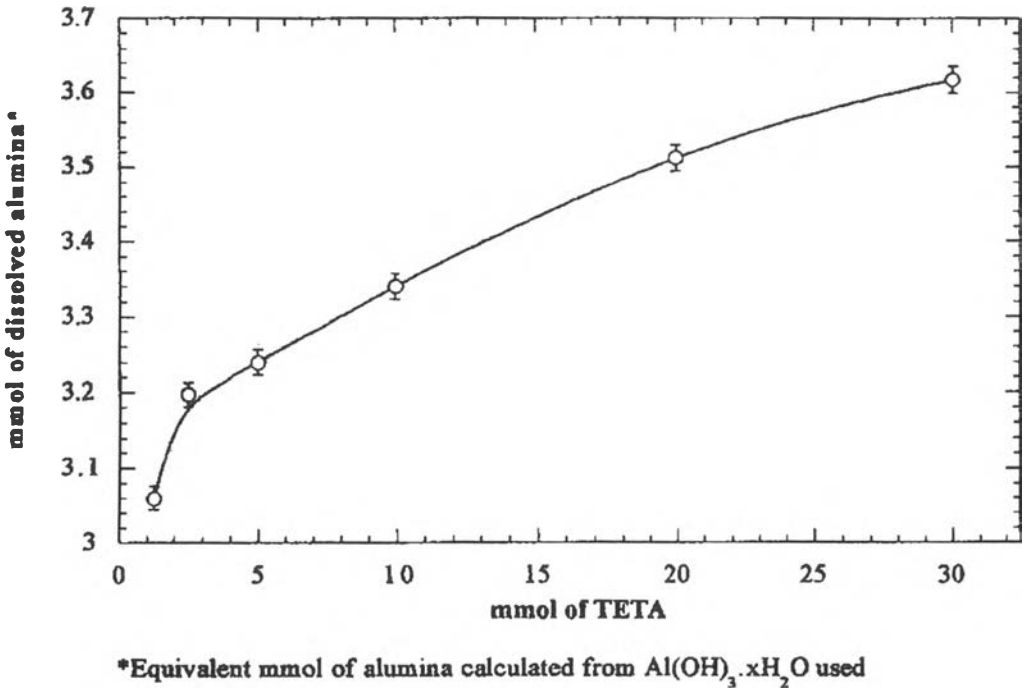

Figure 5. Effect of the TETA concentration.

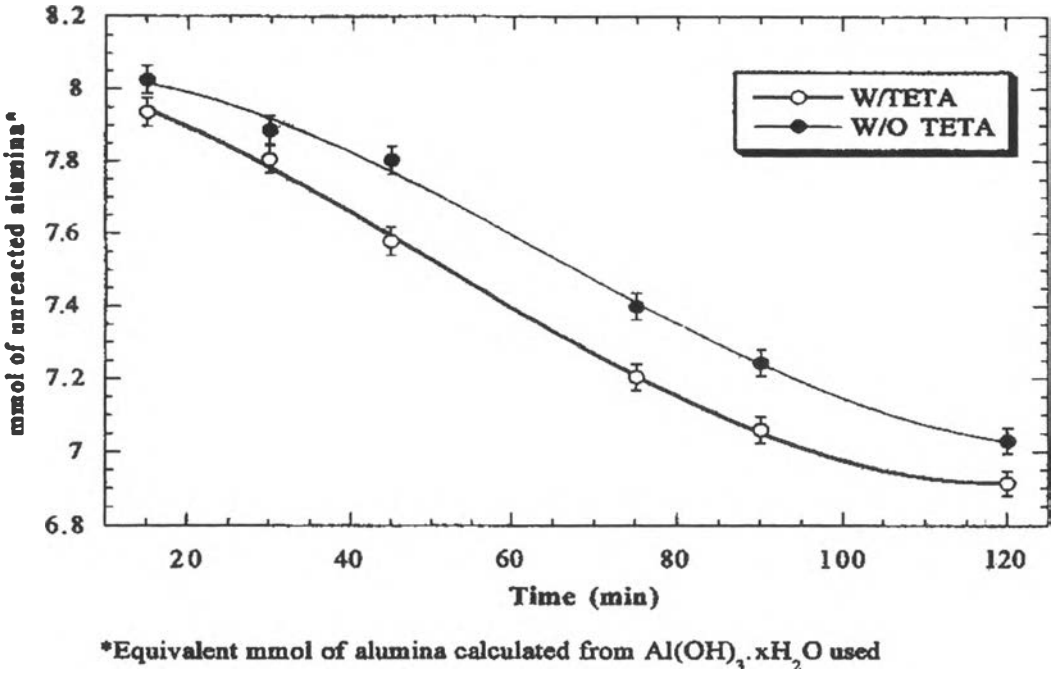

Figure 6. Effect of TETA concentration with time.

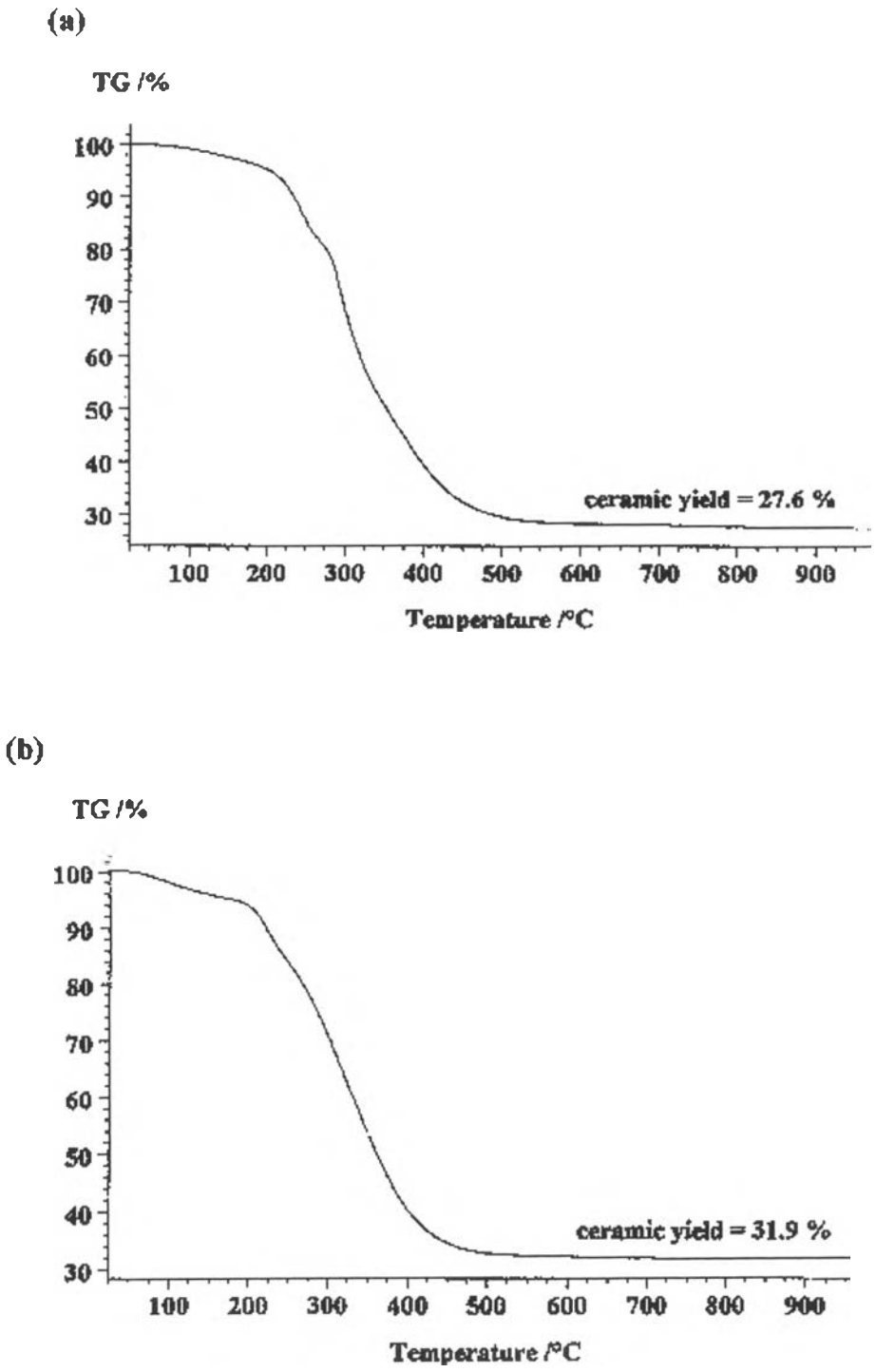

Figure 7. TGA thermogram of the product from the reactions: (a) with and (b) without TETA.

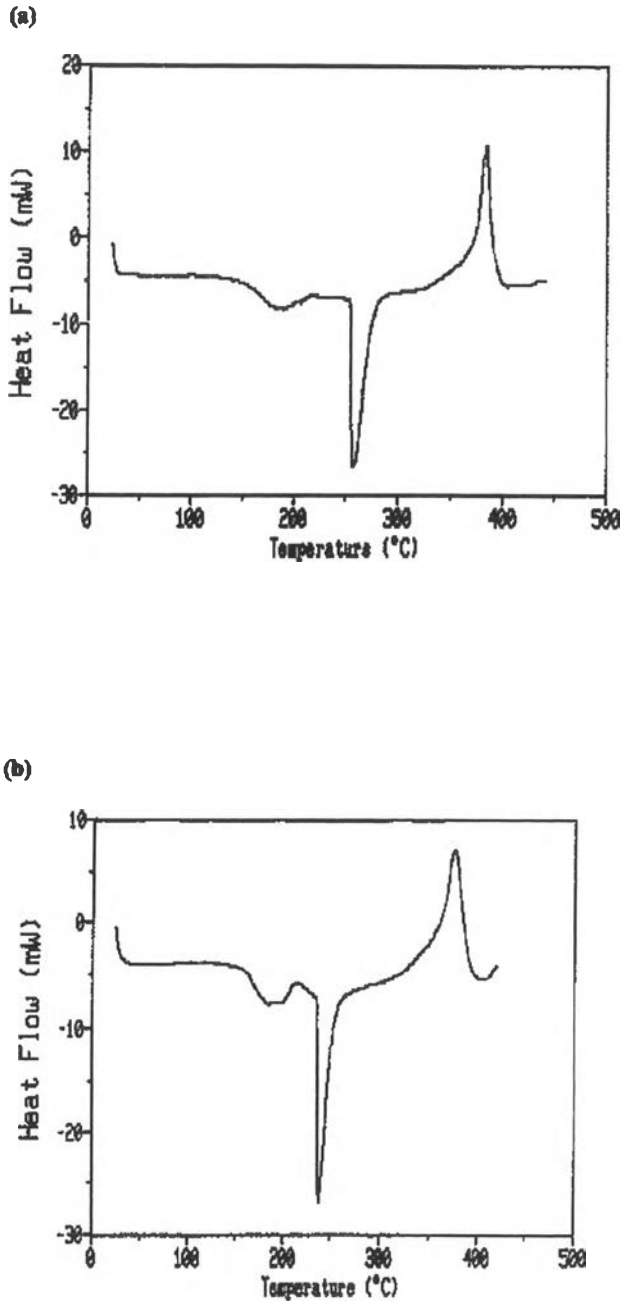

Figure 8. DSC thermograms of the product from the reactions (a) with and (b) without TETA.

Table 1 The Proposed Structures and Fragmentation Pattern of Products

m/e	Intensities	Proposed Structure
216	50	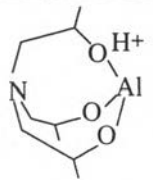 $AlN(CH_2CH_2CH_3O)_3H^+$
409	17.5	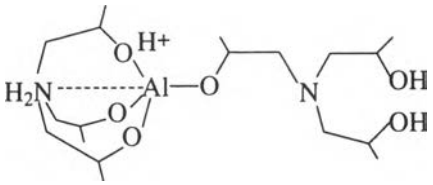 $AlN(CH_2CH_2CH_3O)_3N(CH_2CH_2CH_3O)(CH_2CH_2CH_3OH)_2H^+$
492	38.7	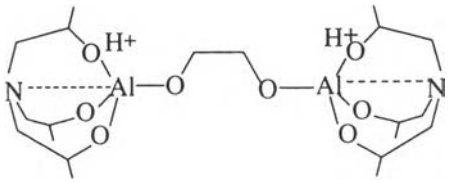 $Al_2[N(CH_2CH_2CH_3O)_3]_2\ (OCH_2\ CH_2O)\ H_2^+$
707	35.4	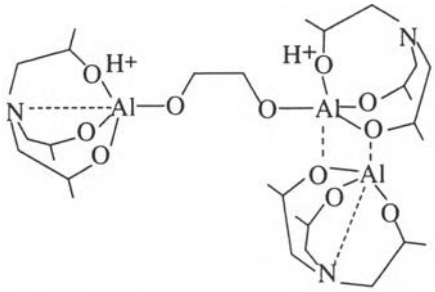 $Al_3[N(CH_2CH_2CH_3O)_3]_2(OCH_2)_2H_2^+$
959	7.9	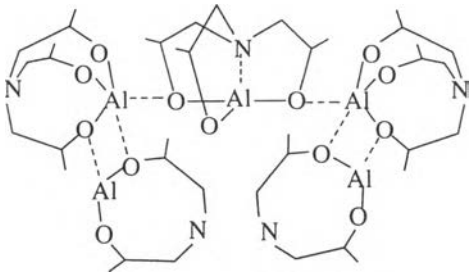 $Al_3[N(CH_2CH_2CH_3O)_3]_2Al_2[N(CH_2CH_2CH_3O)_2]_2$

Table 1 (Con't)

m/e	Intensities	Proposed Structure
1175	46.3	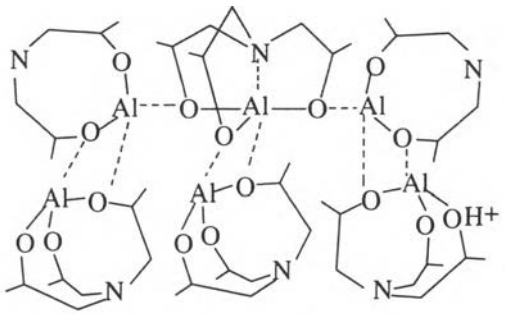 $Al_4(CH_2CH_2CH_3O)_3]_4Al_2[N(CH_2CH_2CH_3O)_2]_2H^+$
1250	100	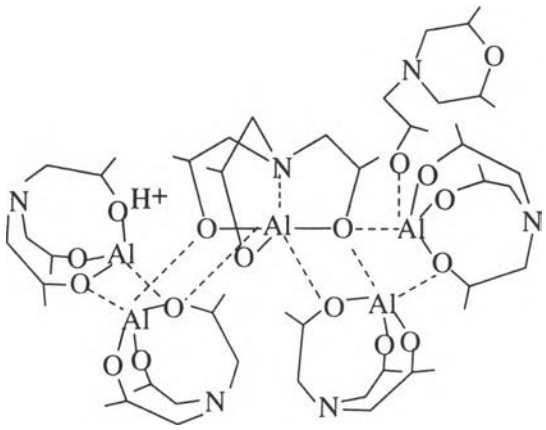 $Al_5[N(CH_2CH_2CH_3O)_3]_5N(CH_2CH_2CH_3O)_2CH_2CH_2CH_3H^+$
1292	7.8	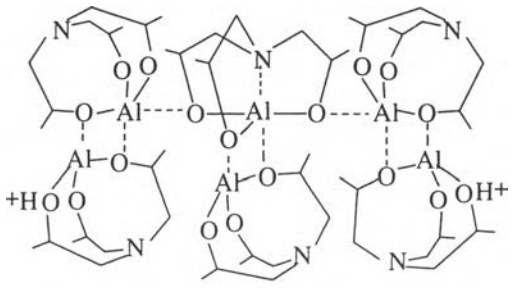 $Al_6[N(CH_2CH_2CH_3O)_3]_6H^+$

Table 2 Peak Positions of ^{1}H- , ^{13}C-, and ^{27}Al-NMR of Products

Compounds	^{1}H-NMR (ppm)	^{13}C-NMR (ppm)	^{27}Al-NMR (ppm)
Product w/o TETA	1.07-1.41 (a) 2.36-3.15 (c) 3.65-4.23 (b)	21.59-22.45 (a) 64.30 (c) 78.56-79.21	7.5 49.6 66.0
Product w/ TETA	1.07-1.88 (a) 2.23-2.85 (c) 3.73-4.11 (b)	20.79 (a) 64.30-65.63 (c) 78.79-79.48 (b)	7.4 48.8 64.9

Table 3 Peak Position and Assignments of FTIR Spectra of Products with/without TETA

Peak positions		Assignments
Al-TIS	TIS-Al-TETA	
3000-3700	3000-3700	u O-H and u C-H
2750-3000	2750-3000	u C-H
1650	1630	O-H overtone; C-H bending
1450	1450	δ C-H
1000-1200	1000-1250	u C-N; O-H bending
500-800	500-800	u Al-O

Appendix B

SOL-GEL PROCESSING OF SILATRANES

Abstract

Silatrane complexes are organosilicon compounds synthesized by direct reaction of SiO_2 and trialkanolamines. Here, we explore their potential as ceramic precursors via the hydrolytic sol-gel processing method. Viscoelastic analysis is used to characterize the gelation behavior of silatranes based on triisopropanolamine, under different hydrolysis conditions. Pyrolysed ceramic products are characterized in terms of surface area and morphology and found to have a homogeneous microporous structure with high surface areas (313-417 m^2/g). Faster hydrolysis rates lead to shorter gelation times, and smaller pore sizes in the derived ceramic.

Introduction

Organosilicate polymers are of interest for their potential as precursors in sol-gel processing to form complex preceramic shapes and structures, not readily accessible by melt processing [1-2]. Due to widespread availability and low cost, silica, (SiO_2) is the ideal starting material to make organosilicon polymers. However, the Si-O bond is very strong and difficult to manipulate chemically [3]. As a corollary, organosilicate polymers, once formed, are very easy to hydrolyze back to SiO_2. Such high reactivity can create problems in chemical processing, therefore it is advantageous to be able to create precursors with reduced hydrolytic activity.

Silatrane complexes are a family of organosilicate compounds derived from reaction of SiO_2 with trialkanolamines such as triethanolamine or triisopropanolamine [4-6]. These materials are hydrolytically stable in air for periods up to several weeks. For this reason, they are candidates for use as precursors in ceramic processing via the sol-gel technique. Here, we report some preliminary viscoelastic studies of sol-gel processing of silatranes under different

hydrolysis conditions, and investigate the characteristics of glasses formed by pyrolysis of the products.

Methods

Synthesis of Silatrane Complex

Materials. Fumed silica (surface area 280 m^2/g, average particle size of 0.007 μm) was purchased from Aldrich Chemical Company, and dried in an oven at 90 °C for 10 hr. Ethylene glycol, purchased from Labscan, was used as reaction solvent, and purified by fractional distillation at 200 °C under N_2 atmosphere. Triisopropanolamine [TIS, $N(CH_2CHCH_3OH)_3$] was obtained from Fluka Chemical Company, and dried in a desiccator. Commercial grade triethylenetetramine [TETA, $H_2NCH_2(CH_2NHCH_2)_2\,CH_2NH_2$], supplied by Union Carbide Thailand, Limited, was purified by vacuum distillation at 120 °C (1mm Hg).

Anhydrous diethyl ether and dichloromethane, used as precipitants, were purchased from Baker Analytical Co. Dichloromethane was distilled over anhydrous calcium chloride under N_2 atmosphere. Anhydrous diethyl ether was dried by adding anhydrous calcium chloride, let stand for 24 hr with occasional shaking, and then filtered into a clean dry bottle. HPLC grade tetrahydrofuran, used as solvent for molecular weight determination by gel permeation chromatography, was purchased from J. T. Baker Inc., and used as received.

Reaction conditions. As discovered by Piboonchaisit [6], silatrane complexes were formed by mixing fumed silica with TIS (and TETA as catalyst) in ethylene glycol (EG) as solvent. The reaction temperature was set at the distillation point of EG (200 °C). Water formed during the reaction, and EG were continuously removed and replaced by an equivalent amount of fresh EG distillate. After reaction, the residual EG was removed by vacuum distillation (1 mm Hg). Based on GPC analysis described below, four distinct chemical species may be formed during the reaction, with proposed structures shown in Fig. 1, whose relative abundance depends on the molar ratio of TIS:SiO_2, the amount of TETA catalyst present, the temperature at which the vacuum distillation of EG is carried out, and on the

duration of this distillation procedure. Of the four structures shown, that with molecular weight 407 is particularly undesirable, because the silicon content is low, and hence the % ceramic yield is poor, which makes the product unsuitable as a ceramic precursor. The optimal reaction condition, at which minimal formation of this species occurs, was found to be at a 1: 1 molar ratio of TIS:SiO_2, (with TETA in the amount of 5 mol% of silica [6]). As the vacuum distillation temperature increases, the amount of high molecular weight species increases up to 180 °C, after which it decreases again, as shown in Fig. 2. The optimum temperature for high ceramic yield is therefore 180 °C.

Characterisation of Silatrane Complexes

FTIR Spectroscopy. FTIR spectroscopic analysis was performed using a Bruker instrument with a resolution of 4 cm^{-1}. Powdered specimens containing 1.0% sample mixed with 99% crystalline KBr were compressed into pellets. The pellets were placed in the sample chamber purged with N_2 for 20 minutes to remove CO_2.

NMR Spectroscopy. ^{13}C and ^{1}H NMR spectra of silatrane complexes were obtained using a 500MHz JEOL spectrometer. Samples were dissolved in deuterated DMSO. Tetramethylsilane was used as the internal reference for both proton and carbon NMR.

Gel Permeation Chromatography. GPC chromatograms were performed using a Waters 600E Instrument equipped with UV and RI detectors (Waters 486 and 410, respectively). The column used was Styragel of pore size suitable to separate molecular weights in the range 0 to 1,000. Calibration was performed using polystyrene standards of narrow molecular weight distribution. THF was the solvent at ambient temperature. The silatrane samples were dissolved in THF at concentration below 0.3% weight, and filtered through 0.45 μm membrane filters prior to GPC analysis.

Rheological determination of the sol-gel transition. The transformation from a sol to a gel can be monitored rheologically by following the change in viscoelastic properties. The silatrane reaction product, after removal of residual ethylene glycol, has the appearance of a hard plastic, and was used without further purification. The material was dissolved in the hydrolysis solvent at a concentration of 150% w/v. The hydrolysis temperature was selected to be 40 °C, 50 °C, or 60 °C. The solution was stirred until homogeneous and preheated in a water bath at the hydrolysis temperature, until the solution was viscous enough to be transferred to the rheometer. The cone and plate attachment of the rheometer was pre-heated to the hydrolysis temperature. The gelation time was determined from the point during pre-heating at which the solution reached the hydrolysis temperature in the water bath. Measurements of storage ($G'(\omega)$) and loss ($G''(\omega)$) moduli were made in a Rheometrics ARES rheometer with a 10g-cm transducer, in cone and plate geometry (cone radius 50 mm, cone angle 0.04 radians). Measurement of $G'(\omega)$ and $G''(\omega)$ was performed at 10 frequencies ω ranging from 0.1 to 1.6 rad/sec. Each frequency scan required 10 sec.

The precise location of the gel point as determined from viscoelastic measurements has been discussed in the previous literature [7]. Initially, the material in the sol state is a viscous fluid such that $\tan\delta = G''(\omega)/G'(\omega) >> 1$. As gelation proceeds, G' and G" increase and, ultimately, the material becomes an elastic gel, $\tan\delta << 1$. Frequently, it is assumed that the gel point occurs at the location of the crossover of the loss (G") and storage (G') moduli (i.e. where $\tan\delta = 1$). However, experimentally, this crossover point is often found to depend on the deformation frequency, ω. A more definitive analysis is now possible following more recent experimental and theoretical work [7-8]. At the gel point, power-law behavior is observed in the frequency dependence of dynamic mechanical experiments. Specifically, the storage and loss moduli follow the relationships [7-8]:

$$G'(\omega) = G''(\omega)/\tan(n\pi/2) = \Gamma(1-n)\cos(n\pi/2)S\omega^n \qquad (1)$$

where $\Gamma(1-n)$ refers to the gamma function of argument (1-n). The phase angle δ between stress and strain is independent of frequency and proportional to the relaxation exponent, n:

$$\delta = n\pi/2 \qquad (2)$$

A variety of experimental studies have been reported [7; 9-12], which support the validity of this viscoelastic definition of the gel point, including both chemically and physically cross-linked systems. Experimental values of the relaxation exponent n vary from $n \cong 0.2$ to $n \cong 0.8$. For certain chemically cross-linked systems, n depends on stoichiometry. Theoretical predictions, which support various values of the dynamical exponent, n, have been reported [7; 13-14]. Physically, the power law dependence of the moduli originates in the fact that the gel point occurs when the first sample-spanning gel cluster forms. Hence, the magnitude of the dynamical exponent is determined by the structure and hydrodynamic properties of the critical cluster. The power-law behavior originates in the fact that the structure of the critical gel has a fractal character [14].

Characterisation of Pyrolysis Products

BET Surface Area Measurement. The surface area of pyrolysed polysilatrane gels was determined using an Autosorb-1 Gas Sorption System (Quantachrome Corporation) via the Brunauer-Emmett-Teller (BET) method. A gaseous mixture of nitrogen and helium was allowed to flow through the analyser at a constant rate of 30 cc/min. Nitrogen was used to calibrate the analyser, and was also used as the adsorbate at liquid nitrogen temperature. Each sample was degassed at 300 ^{o}C for 2 hr before analysis. The surface area was obtained from a five-point isotherm at P/P_o ratio less than 0.3. The results were computed based on the desorption surface area and the dried weight of the sample after analysis.

Scanning Electron Microscopy. SEM micrographs were obtained using a JEOL 5200-2AE(MP 15152001) scanning electron microscope. Samples were prepared for SEM analysis by attachment to Aluminum stubs, after pyrolysis at 800

°C. Prior to analysis, the specimens were dried in a vacuum oven at 70 °C for 5 hr, and then coated with gold by vapor deposition. Micrographs of the pyrolysed sample surfaces were obtained at 2,000 and 7,500 magnification.

Results and Discussion

Structural Characterisation of Silatrane Complex. Silatrane complexes produced by the synthetic method described above are a mixture of four molecular species, based on GPC analysis. Proposed structures of each species are shown in Fig. 1. Evidence for the formation of silatrane complexes includes observation of characteristic absorption bands in FTIR analysis (Table 1) and resonance frequencies in ^{13}C and ^{1}H NMR spectroscopy (Table 2).

Rheological analysis of Sol-Gel transition of Silatranes. Silatrane complex formed after vacuum distillation of ethylene glycol was dissolved in one of three hydrolysis solvents at a concentration of 150 % w/v. The hydrolysis solvents were: distilled de-ionized water with measured pH = 6.7; MgO solution prepared by dissolving 0.5 g MgO in 1 liter distilled de-ionized water with measured pH = 11.3; and a solution of methanol in distilled de-ionized water at a ratio 1:1 (pH = 8.1). The change in G' and G" was observed following procedures described above. In Fig. 3, we show frequency scans of G' and G" during hydrolysis in water at 40 °C at three times, viz. before the gel point, at the gel point, and after the gel point. The location of the gel point was identified following the discussion of Chambon and Winter [7], summarized above in equations (2) and (3), as the point where G' and G" follow the same power law with exponent n, i.e. a frequency-independent tanδ. As evident in Fig. 4, this occurs at gel time t = 15600 s ± 1100 s, when n ~ 1.0 and tan δ ~ 1.0. The corresponding variation of tanδ, the apparent frequency exponents of G' and G", and the change in magnitude of the dynamic viscosity, $\eta^*(\omega)$, during hydrolysis are shown in Figs. 4, 5, and 6, respectively. As evident in Figs. 4 and 5, there is considerable uncertainty (~± 7%) in deciding the location of the gel point based on the frequency-independence of tanδ, and, therefore, a corresponding uncertainty in

the precise values of the dynamic exponent n = 0.55 ± 0.15. Fig. 6 confirms that, as expected, the dynamic viscosity increases dramatically at the gel point and, after gelation, exhibits a strong dependence on deformation frequency.

Hydrolysis experiments were carried out at three temperatures, and the gel times determined are tabulated in Table 3. At each temperature, as illustrated by Roy and McCarthy [15-16], the shortest gel times are observed in the most ionic MgO solvent, where the hydrolysis rate is fastest, and the longest gel times are in the least ionic MeOH solvent, which has the slowest hydrolysis rate. Also increase of temperature increases the rate of hydrolysis and thus decreases the gel times.

Characterization of pyrolyzed ceramics. Polysilatrane gels produced via hydrolysis in the three solvents at 40 °C were pyrolyzed at various temperatures in the range 200 °C to 800 °C. FTIR spectra are shown in Fig. 7 and indicate increasing conversion to silica, with increasing temperature such that at 800 °C, essentially pure SiO_2 is obtained. Thus pure ceramic product can be generated in high yield, using processing temperatures as low as 800 °C. The surface areas of ceramics produced by pyrolysis at 800 °C of gels formed in each of the hydrolysis solvents at 40 °C were determined by the BET method. The results are listed in Table 4, and indicate a trend of decreasing surface area with decreasing gel times. At high rates of gelation, it is likely that smaller gel particles are formed, which might lead to smaller pore sizes, and hence higher surface areas in the pyrolysed products. In Fig. 8, we show SEM micrographs, taken at a magnification of x7500, of the surfaces of the three pyrolyzed ceramics together with that of the fumed silica starting material. Clearly, sol-gel processing via formation of silatrane complexes has converted the silica from a granular porous solid into a homogeneous microporous glass, with a corresponding increase in surface area from 280 m^2/g to ~ 410 m^2/g. From the micrographs, there appears to be a tendency towards smaller pore sizes with shorter gel times. In particular the ceramic from the MgO hydrolysis solvent has the most finely divided morphology, but shows evidence of contamination by small amounts of precipitated MgO on the surface.

Conclusions

The optimal reaction mixture for silatrane synthesis is one with equimilar amounts of TIS and SiO_2 in the presence of 5 mol% of silica. The optimum vacuum distillation temperature is 180 °C. After 12 hours under these conditions, most of the solvent is removed, and the monomer (M = 277) is largely converted to the dimer with M = 492. Gelation of the silatrane complex formed under these conditions is achieved by hydrolysis under ionic conditions. Pyrolysis of the gels at 800 °C produces a homogeneous microporous glass. Glass formed under more ionic conditions (MgO/H_2O) has the smallest pores and largest surface area, but suffers from contamination by precipitated MgO.

References

1. Saegusa, T. and Chujo, Y., , *Advance Polymer Science* **1992**, *100*, 11.
2. Varshneya, A., *Fundamentals of Inorganic Glassmaking* **1994**, Boston:Academic Press.
3. Iler, R., *The Chemistry of Silica* **1979**, NewYork: John Wiley & Sons.
4. Hencsei, P. and Parkanyi, L., *Review Silicon, Germenium, Tin Lead Compound* **1985**, *8(2)*, 191.
5. Bickmore, C., Hoppe, M. and Laine, R., *Material Research Society Symposia Processing* **1992**, *249*, 81.
6. Piboonchaisit, P., Wongkasemjit, S. and Laine, R., *ScienceAsia, J.Sci.Soc. Thailand* **1999**, *25*, 113.
7. Winter, H. and Chambon, F., *J. Rheol.* **1986**, *30*, 367.
8. Muthukumar, M. and Winter, H., *Macromolecules* **1986**, *19*, 1284.
9. Hodgson, D., Qun, Y. and Amis, E., *J. Non-Crst. Solids* **1991**, *131-133*, 913.
10. Muller, R., Gerard, E., Dugand, P., Rempp, P. and Gnanou, Y., *Macromolecules* **1991**, *21*, 532.
11. Izuka, A., Winter, H. and Hashimoto, T., *Macromolecules* **1992**, *25*, 2422.
12. Hsu, S. and Jamieson, A., *Polymer* **1993**, *34*, 2601.
13. Lin, Y., Mallin, D., Chien, J. and Winter, H., *Macromolecules* **1991**, *24*, 850.
14. Muthukuma, M., *Macromolecules* **1989**, *22*, 4656.
15. Roy, R., *J. Amer. Cer. Soc.* **1969**, 344.

16. McCarthy, G. and Roy, R., *J. Amer. Cer. Soc.* **1971**, 639.

Table 1 Assignments of infrared spectra of the products.

Characterization	Silatrane Complexes
Si-N stretching[a]	560-590 cm^{-1}
Si-O-CH[b]	970,883 cm^{-1}
C-O[a]	1013-1070 cm^{-1}
Si-O-CH_2[b]	1015-1085 cm^{-1}
C-N[a]	1270 cm^{-1}
C-H bending[a]	1380-1460 cm^{-1}
C-H stretching[a]	2800-29760 cm^{-1}

a: Silverstein *et al.* 1991.

b: Anderson D.R., 1974.

Table 2 ^{1}H-and ^{13}C-NMR chemical shifts of silatrane complexes

Position	Groups	^{1}H-NMR (ppm)	^{13}C-NMR (ppm)
(a)	N-C<u>H</u>$_2$	2.86-2.91	57.7
(b)	CH-C<u>H</u>$_3$	4.0	23
(c)	C<u>H</u>-CH$_3$	0.96-1.12	20-21
(d)	C<u>H</u>$_2$-O	3.3	59.2
(e)	C<u>H</u>$_2$-OH	3.4-3.5	62.5-65

Table 3 Viscoelastic properties at the sol-gel transition of polysilatrane.

Solvent	**Temperature (°C)**	**Gelling time(s)**	**tanδ**	***n***
MgO + H_2O	60	4500	1.31	0.55
H_2O	60	6620	1.62	0.75
MeOH + H_2O	60	8260	1.20	0.61
MgO + H_2O	50	8950	3.02	0.85
H_2O	50	9350	2.24	0.79
MeOH + H_2O	50	9560	0.98	0.49
MgO + H_2O	40	14567	1.20	0.62
H_2O	40	16200	1.06	0.53
MeOH + H_2O	40	18892	1.42	0.67

Table 4 Surface area of polysilatrane gel pyrolyzed at 800°C

Gel	Surface area (m^2/g)
Hydrolyzed MgO+ H_2O	417
Hydrolyzed H_2O	401
Hydrolyzed MeOH+H_2O	313
Pyrolyzed start from 500°C	414
Pyrolyzed start from room temp.	388

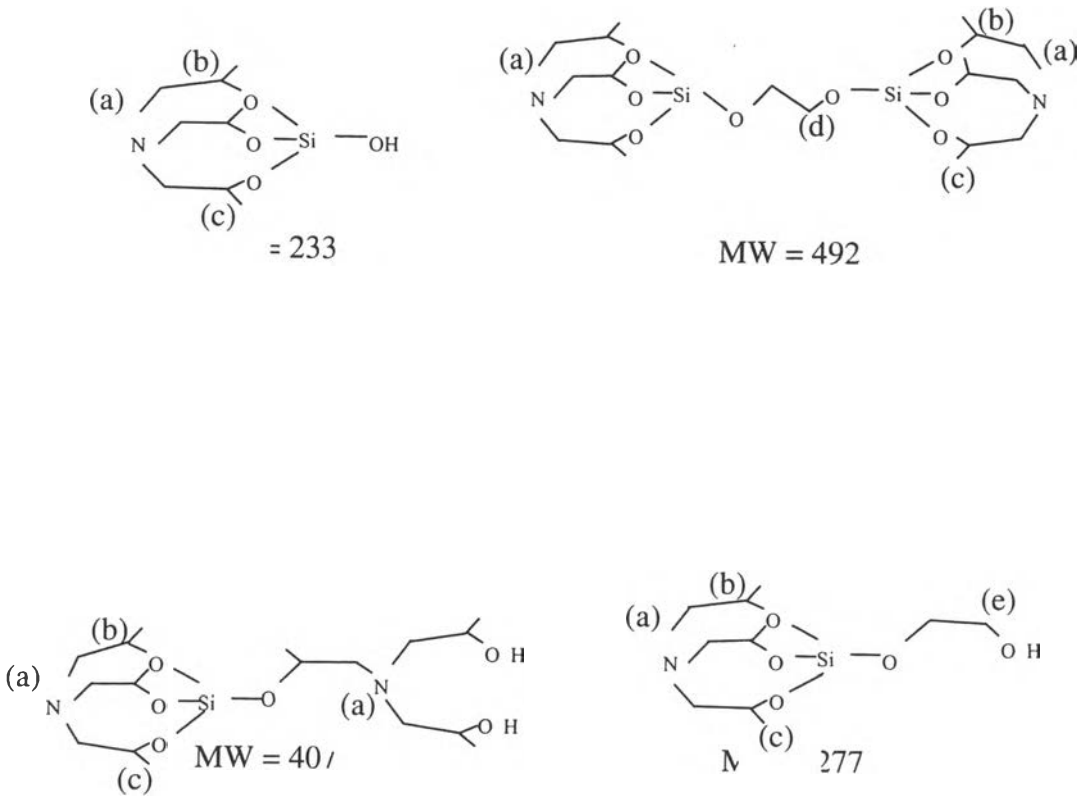

Figure 1 The proposed structures of silatrane complexes using 1:1 ratio of [TIS]: [SiO_2].

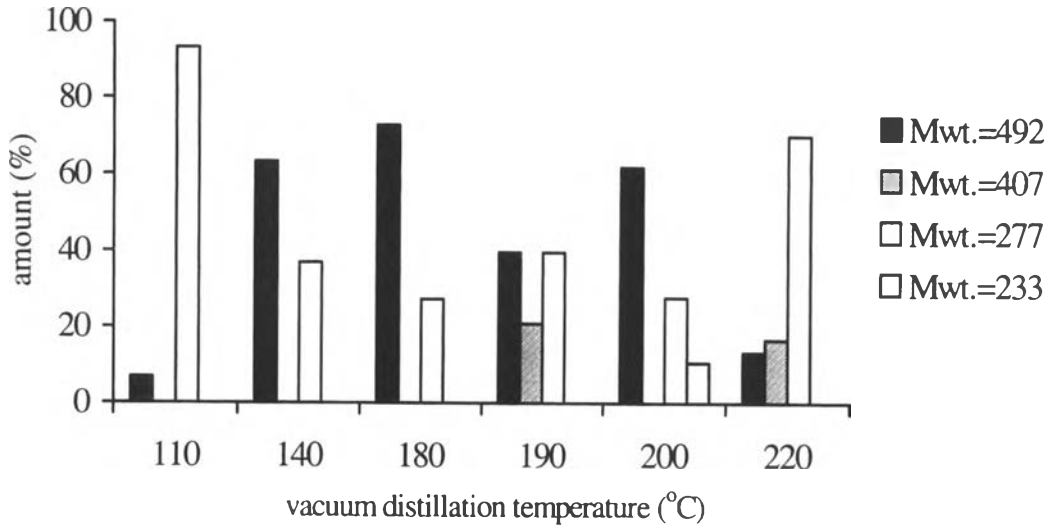

Figure 2 Silatrane complexes obtained at 1:1 [TIS]:[SiO_2] and various vacuum distillation temperature.

Before gel point

$n''>n'$

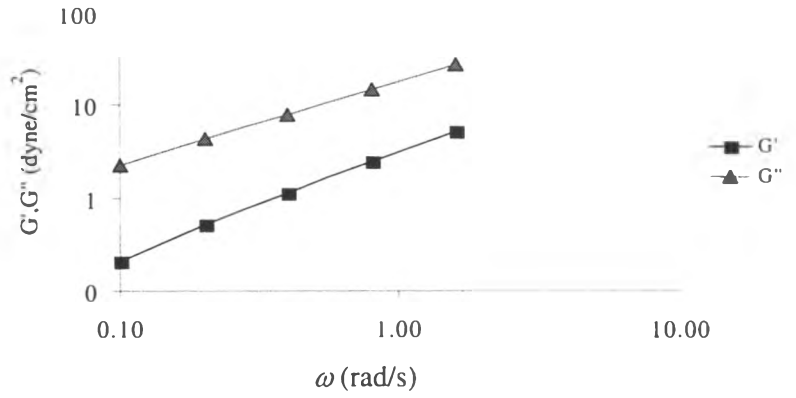

Gel point

$n'=n''$

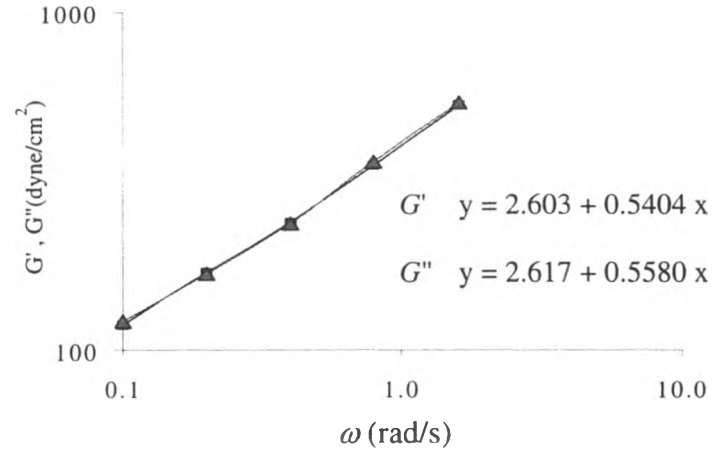

After gel point

$n'>n''$

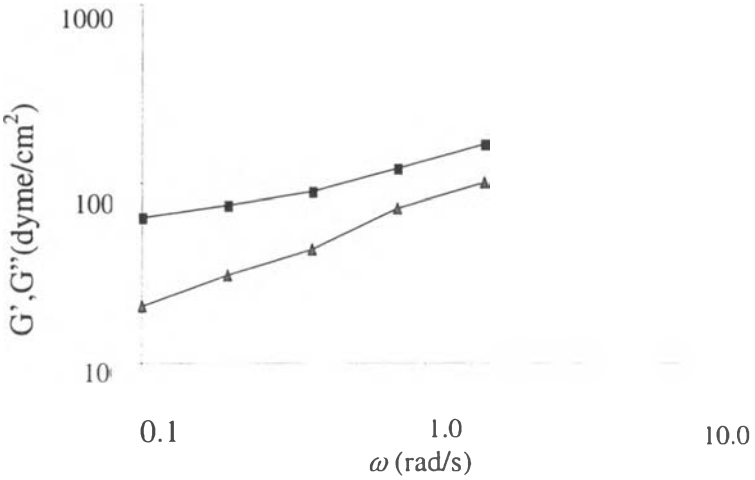

Figure 3 The relationship of log G' and G'' vs. log frequency of 150 % w/v silatrane complex hydrolyzed in water at $T = 40^{\circ}C$

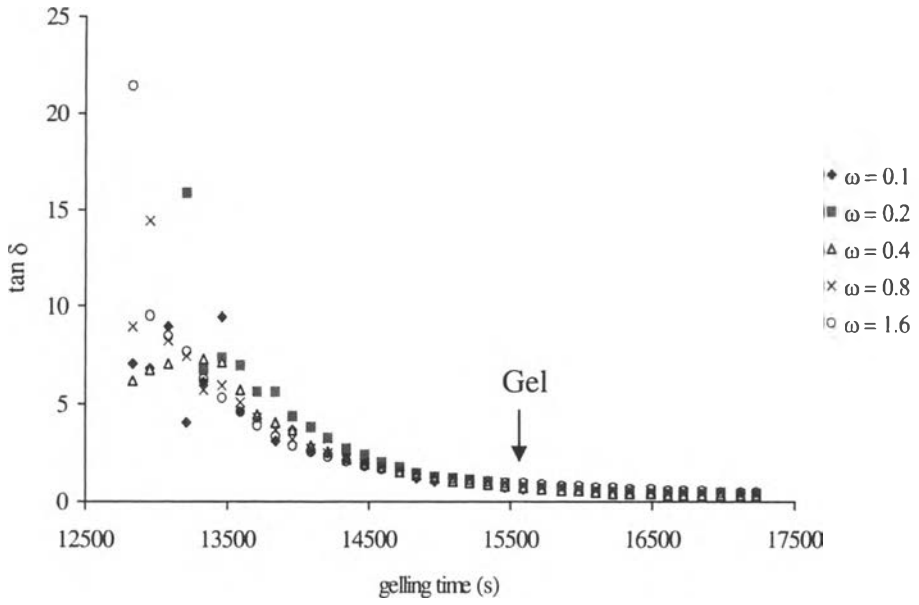

Figure 4 Multi-frequency plot of tanδ vs. gelling time of 150 % w/v silatrane complex hydrolyzed in water at $T = 40$ °C

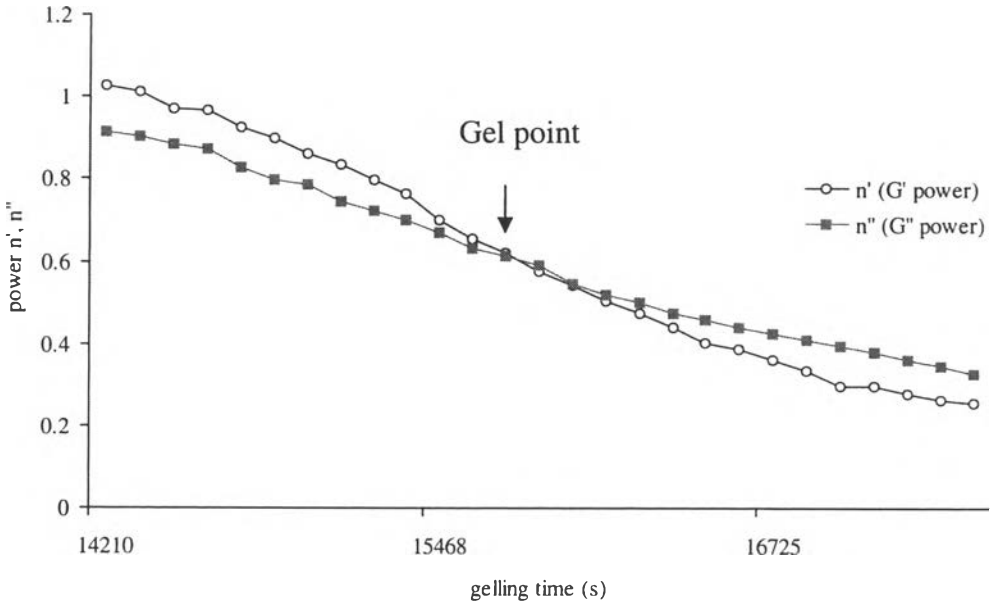

Figure 5 The plot of power-law exponent n' and n" vs. gelling time of 150 % w/v silatrane complex hydrolyzed in water at $T = 40\ ^{o}C$

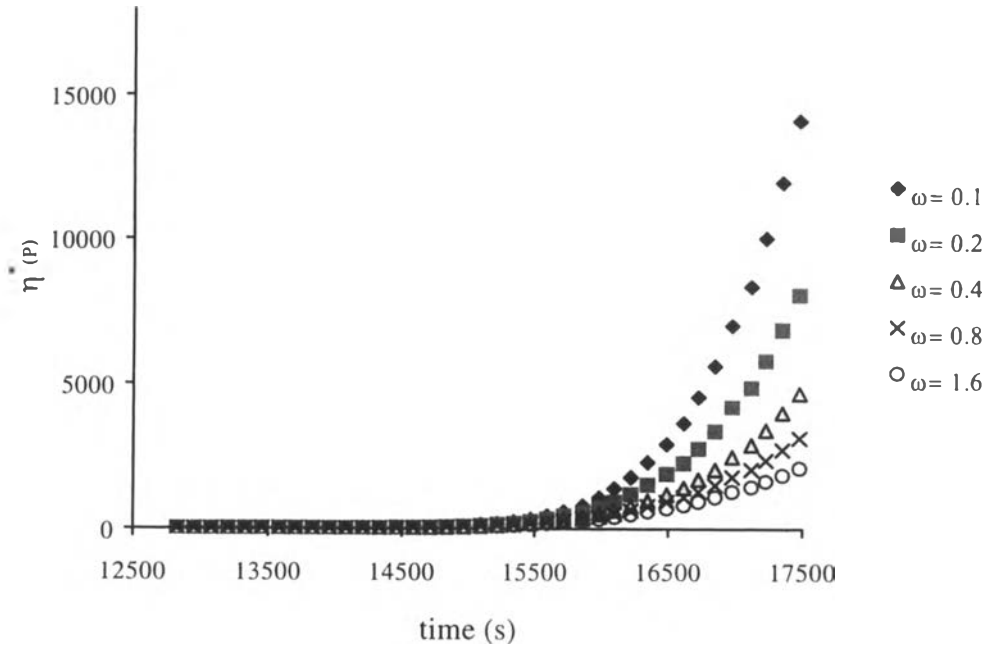

Figure 6 Complex viscosity (η^*) at different frequency plotted vs. gelling time of 150 % w/v silatrane complex hydrolyzed in water at $T = 40$ °C

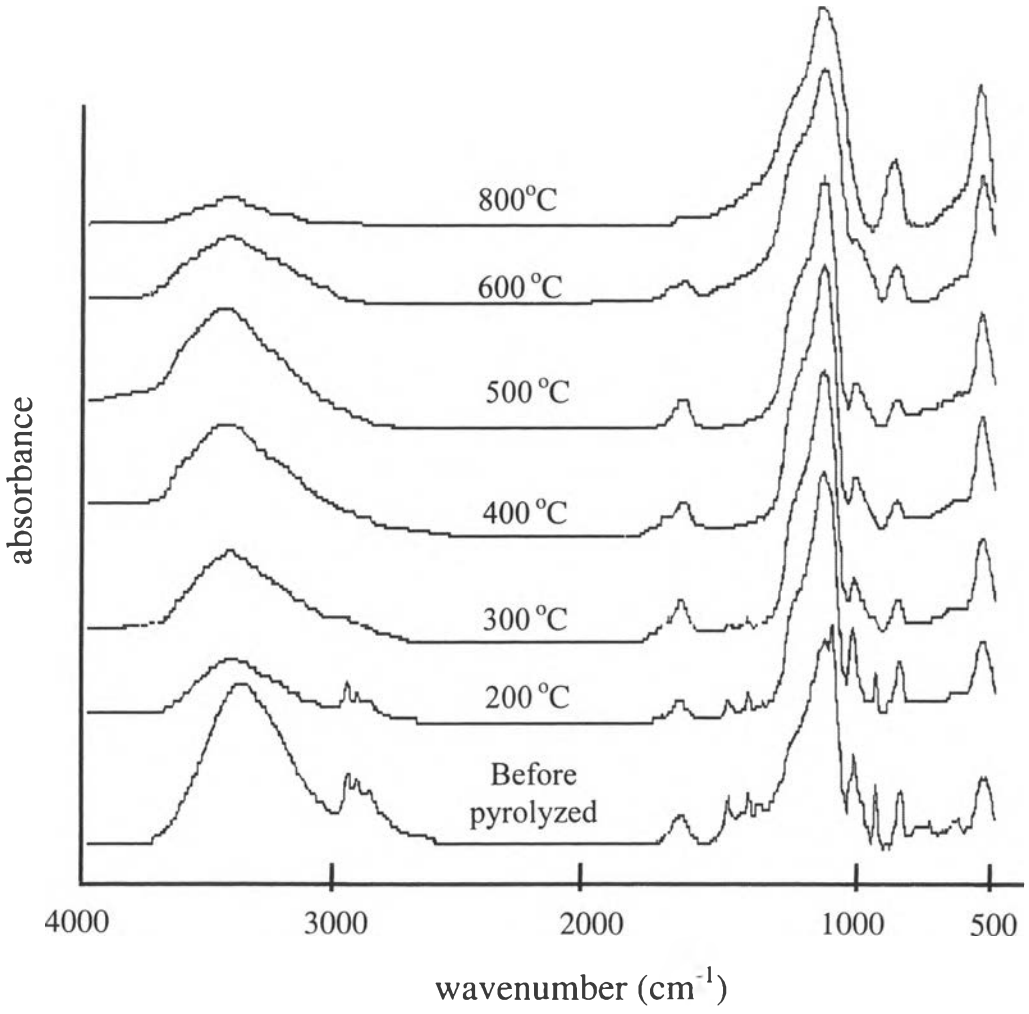

Figure 7 FTIR spectra of the pyrolyzed polysilatrane gel at different temperatures.

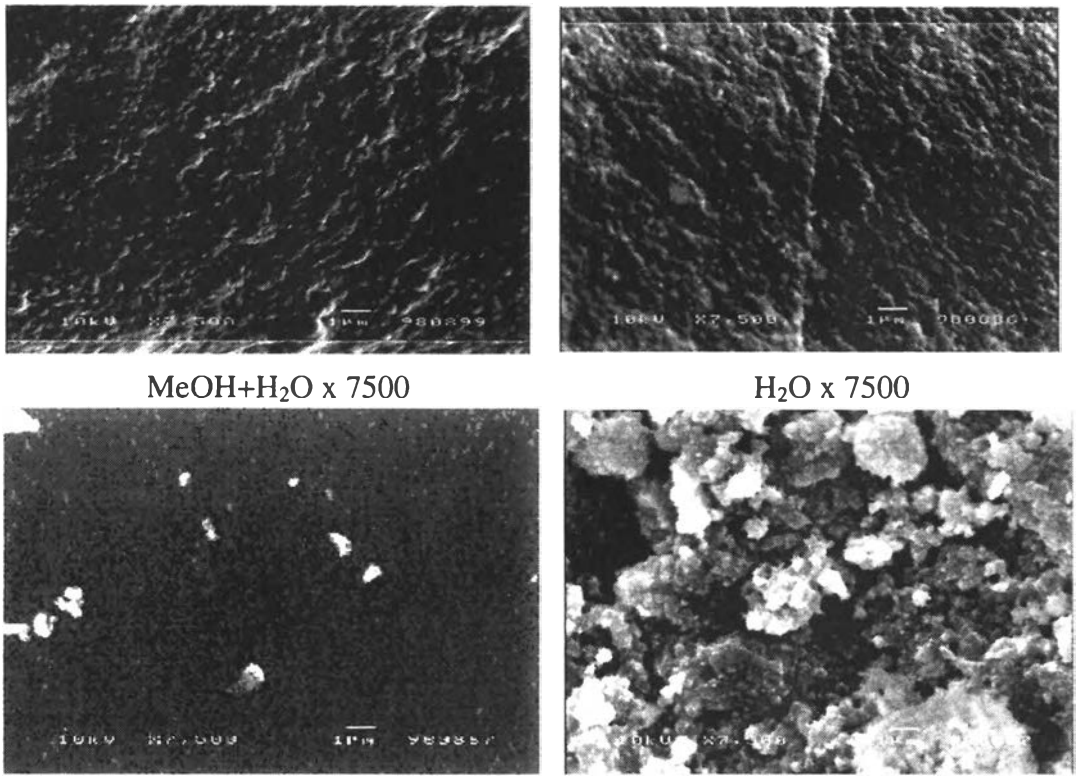

MeOH+H_2O x 7500 H_2O x 7500

MgO+H_2O x 7500 Fumed SiO_2 x 7500

Figure 8. SEM micrograph of pyrolyzed polysilatrane hydrolyzed with various solvent, at 800 °C, and heating rate of 10 °C/min as compared with fumed SiO_2 with magnification 7500

CURRICULUM VITAE

Name: Ms. Bussarin Ksapabutr

Date of Birth: September 4, 1974

Nationality: Thai

University Education:

1992-1996 Bachelor Degree of Science in Materials Technology, Faculty of Engineering and Industrial Technology, Silpakorn University, Nakornpathom, Thailand.

Working Experience:

1996-1998 Position: Instructor

University: Silpakorn University

Publications:

1. Y. Opornsawad, B. Ksapabutr, S. Wongkasemjit, R.M. Laine, Formation and structure of tris(alumatranyloxy-i-propyl)amine directly from $Al(OH)_3$ and triisopropanolamine, *European Polymer Journal* , **2001**, *37*, 1877-1885.
2. W. Charoenpinijkarn, B. Ksapabutr, S. Wongkasemjit, A.M. Jamieson, Sol-gel processing of silatranes, *European Polymer Journal* , **2001,** *37*, 1441-1448.
3. B. Ksapabutr, S. Wongkasemjit, E. Gulari, One-pot synthesis and Characterization of novel sodium tris(glycozirconate) and cerium glycolate precursors and their pyrolysis. *Mater. Chem. Phys.*, **2004**, *83*, 34-42.
4. B. Ksapabutr, S. Wongkasemjit, E. Gulari, Sol-gel transition study and pyrolysis of alumina based gels prepared from alumatrane precursor. *Colloids and Surfaces A: Physicochem. Eng. Aspects*, **2004**, 233, 145-153
5. B. Ksapabutr, S. Wongkasemjit, E. Gulari, Rheology and heat treatment of zirconia based gels synthesized from sodium glycozirconate precursor. [Submitted to *Journal of Non-Crystalline Solids*]

6. B. Ksapabutr, S. Wongkasemjit, E. Gulari, Preparation of zirconia powders by sol-gel route of sodium tris(glycozirconate) complex. [Submitted to *Colloids and Surfaces A: Physicochemical and Engineering Aspects*]
7. B. Ksapabutr, S. Wongkasemjit, E. Gulari, Preparation of zirconia powders by sol-gel route of sodium tris(glycozirconate) complex. [Submitted to *Microporous and Mesoporous Materials*]

Proceedings:

1. B. Ksapabutr, S. Wongkasemjit, E. Gulari, Rheology and heat treatment of zirconia based gels synthesized from sodium glycozirconate precursor, The First International Meeting on Applied Physics (APHYS-2003), 2003, Badajoz, Spain.
2. B. Ksapabutr, S. Wongkasemjit, E. Gulari, Preparation of zirconia powders by sol-gel route of sodium tris(glycozirconate) complex. The First International Meeting on Applied Physics (APHYS-2003), 2003, Badajoz, Spain.

Presentations:

1. B. Ksapabutr, S. Wongkasemjit, E. Gulari, Rheology and heat treatment of zirconia based gels synthesized from sodium glycozirconate precursor, The First International Meeting on Applied Physics (APHYS-2003), 2003, Badajoz, Spain.
2. B. Ksapabutr, S. Wongkasemjit, E. Gulari, Preparation of zirconia powders by sol-gel route of sodium tris(glycozirconate) complex. The First International Meeting on Applied Physics (APHYS-2003), 2003, Badajoz, Spain.